

in Figure 2, Figure 3 and Figure 4. Sides of rain garden are enclosed with vertical acrylic sheet to prevent outside flow of water from rain garden.

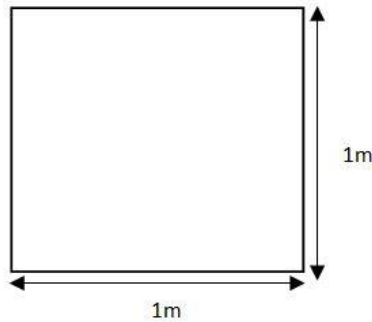


Figure 2. Rain garden 1 (Flat)

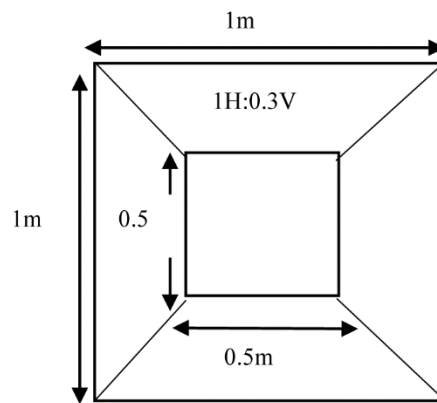


Figure 3. Rain garden 2 (slope 1H:0.3V)

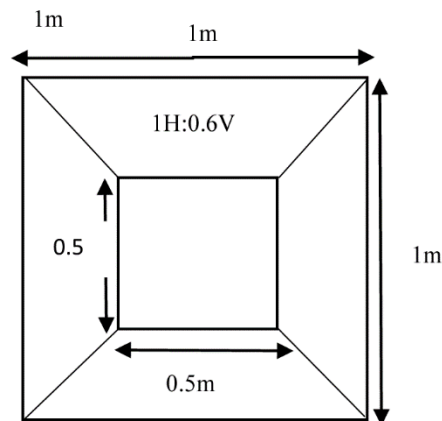


Figure 4. Rain garden 3 (slope 1H:0.6V)

Experiment

A cylindrical storage tank of capacity 170 litres is provided near the rain gardens. Watering of rain garden is done with a polyvinyl chloride pipe connected to the storage tank (Figure 5). To study the effect of slope profile of rain garden on rate of infiltration we will add the same volume of water in all the three rain gardens and note time in which the given volume of water infiltrates. The rain garden in which water infiltrates quickly is the most suitable profile for the rain garden.

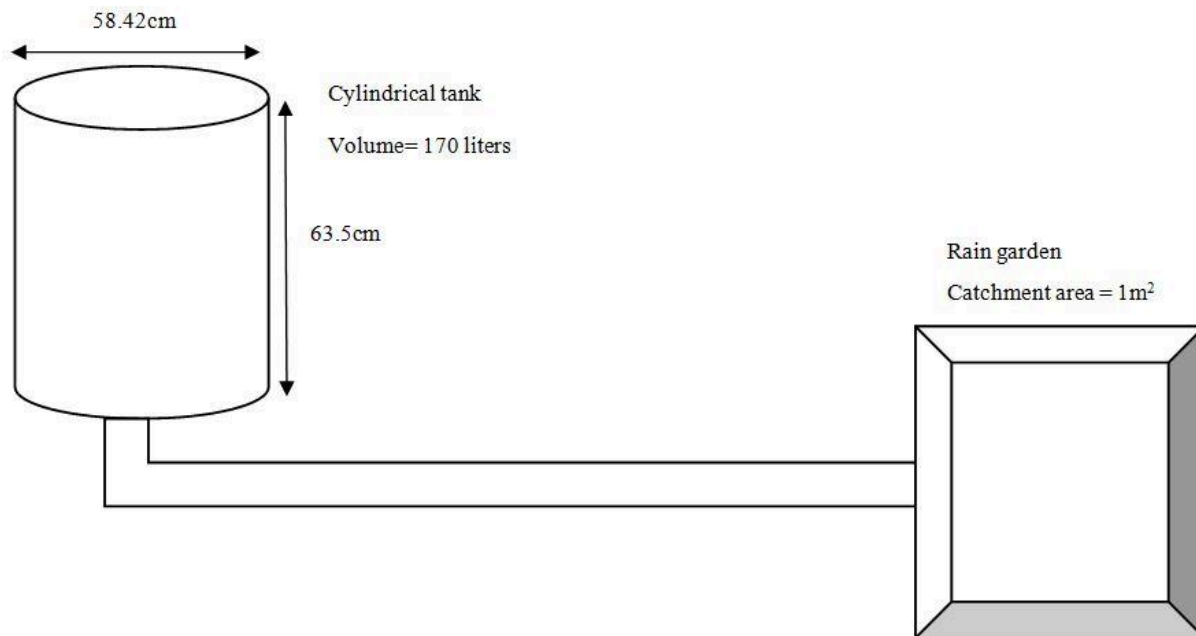


Figure 5. Outline of experimental site used for watering of rain garden

Vegetation in Rain Garden

Scutch grass (*Cynodon dactylon*) is planted in all the three rain gardens. The number of grass plants in a rain garden is 140. This is the native vegetation of the region. This kind of grass requires very less irrigation and is most suitable for rain gardens. Vegetation helps in increasing the infiltration rate of soil (Li et al. 2016). Vegetation helps in reducing the volume of water by process of evaporation and transpiration (Yuan et al. 2017).

RESULTS AND DISCUSSIONS

Soil in Rain gardens

The initial exploration during construction of rain gardens includes a visual description and field soil texture, which recognized the soil as a clayey loam, brown in color. To get the detail properties of in-situ soils, additional tests on soil were conducted. The tests conducted on soil were not a consideration for location or design of rain gardens; rather, they were solely based on the properties of soil that may influence the gardens hydraulic properties. The tests conducted on soil were Atterberg limit Particle size distribution. The results of the tests are presented in Table 1. The soil is found to be a Clayey Sand, as defined in Unified Soil Classification system.

Table 1. The results of the in-situ soil tests

Particle Size Distribution		Atterberg Limits	
Sand (75-425 μ)	54.38%	Liquid Limit	24.10 %
		Plastic Limit	15.16 %
Clay ($\leq 2\mu$)	45.62%	Plasticity Index	8.93 %

During the experiment, the storage tank supplied the water to rain garden. Initially, 50 litres of water were added to all the three rain gardens. The discharge was kept 4.54 litres/minute for all the three rain gardens. The storage tank was placed 60 cm above the ground. As same volume of water is added in all the three rain gardens, time is noted in which the water infiltrates in the garden. The results (Table 2) clearly indicate that in flat profile water infiltrates out most quickly. The water stands for maximum time in rain garden with slope 1H:0.6V. Standing of water leads to mosquito breeding and is aesthetically displeasing. So flat rain garden is most suitable profile for a rain garden.

Table 2. Time consumed in infiltrating 50 litres of water with 8cm height of grass in rain gardens

Observation	Time of observation	Temperature	Mean discharge (litre/min)	Rain garden 1 (seconds)	Rain garden 2 (seconds)	Rain garden 3 (seconds)
Observation 1	15 Sep 2017	36°C	4.54	600	1320	2700
Observation 2	10 Oct 2017	33°C	4.54	610	1365	2852
Observation 3	21 Nov 2017	25°C	4.54	730	1450	3000
Observation 4	22 Dec 2017	22°C	4.54	794	1550	3327
Observation 5	5 Jan 2017	12°C	4.54	880	1630	3590

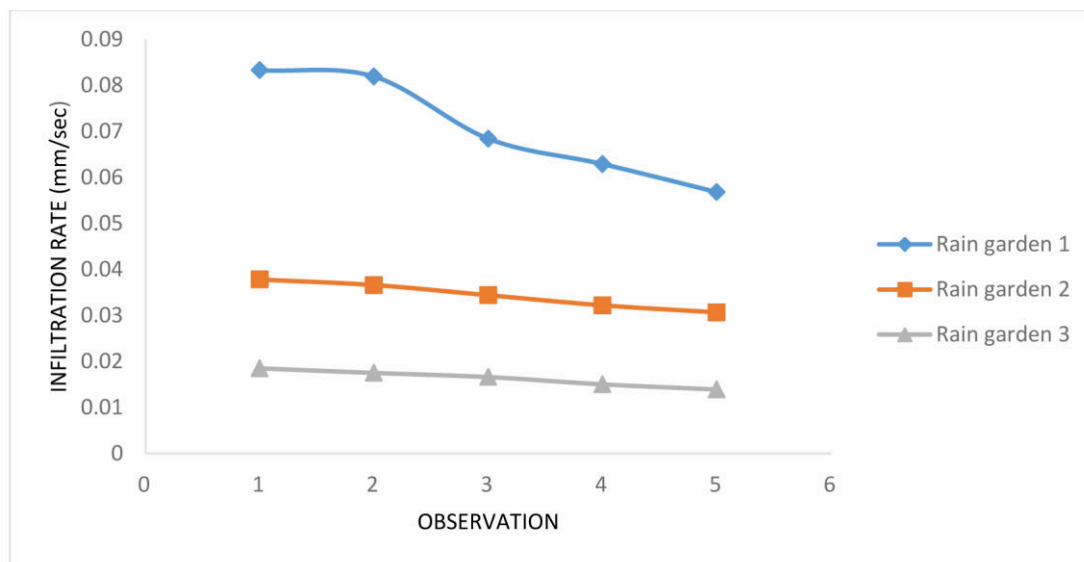


Figure 6. Comparative of infiltration rate of rain gardens and effect of temperature on infiltration rate

The curve (Figure 6) clearly indicates that in all the observations, the rate of infiltration is maximum in Rain garden 1 and minimum in Rain garden 3. Also, the rate of infiltration of all the gardens decreases with decrease in temperature of surroundings and the maximum decrease occurs for Rain garden 1.

CONCLUSIONS

The rapid urbanization has become major issues all around the world. Urbanization, besides having adverse impacts on hydro-climatic conditions, has led to a rapid increase in the impervious area. This seals the upper soil layers and thus generates excessive surface runoff causing urban floods. Rain garden, which is considered a low impact development technique, has emerged as a solution to the problem of urban flooding. The influence of slope profile on the hydrological performance of a rain garden was investigated in this study through laboratory experiments considering three rain gardens with different slopes. From the experimental observations, it is concluded that the shallow excavated flat profile rain garden planted with native grass with no outlet is most suitable for rain garden's optimal hydrologic performance.

REFERENCES

- Aadhar, S., Swain, S., and Rath, D. R. (2019). "Application and Performance Assessment of SWAT Hydrological Model over Kharun River Basin, Chhattisgarh, India." In: *World Environmental and Water Resources Congress 2019: Watershed Management, Irrigation and Drainage, and Water Resources Planning and Management*, ASCE, 272-280. <https://doi.org/10.1061/9780784482339.028>
- Aravena, J. E., and Dussailant, A. (2009). "Storm-water infiltration and focused recharge modeling with finite-volume two-dimensional Richards equation: Application to an experimental rain garden." *Journal of Hydraulic Engineering*, 135(12), 1073–1080.
- Blecken, G. T., Zinger, Y., Deletić, A., Fletcher, T. D., and Viklander, M. (2009). "Influence of intermittent wetting and drying conditions on heavy metal removal by stormwater biofilters." *Water research*, 43(18), 4590–4598.
- Carpenter, D. D., and Hallam, L. (2009). "Influence of planting soil mix characteristics on bioretention cell design and performance." *Journal of Hydrologic Engineering*, 15(6), 404–416.
- Chang, N. B. (2010). "Hydrological connections between low-impact development, watershed best management practices, and sustainable development." *Journal of Hydrologic Engineering*, 15(6), 384–385.
- Cosgrove, Jr, J. F., and Bergstrom, J. D. (2003). "Design and construction of biofiltration basins: lessons learned." In: *World Water & Environmental Resources Congress 2003*, pp. 1–10.
- Davis, A. P., Hunt, W. F., Traver, R. G., and Clar, M. (2009). "Bioretention technology: Overview of current practice and future needs." *Journal of Environmental Engineering*, 135(3), 109–117.
- Davis, A. P., Shokouhian, M., Sharma, H., and Minami, C. (2001). "Laboratory study of biological retention for urban stormwater management." *Water Environment Research*, 73(1), 5–14.
- Davis, A. P., Traver, R. G., Hunt, W. F., Lee, R., Brown, R. A., and Olszewski, J. M. (2011). "Hydrologic performance of bioretention storm-water control measures." *Journal of Hydrologic Engineering*, 17(5), 604–614.
- Dayal, D., Swain, S., Gautam, A. K., Palmate, S. S., Pandey, A., and Mishra, S. K. (2019). "Development of ARIMA Model for Monthly Rainfall Forecasting over an Indian River Basin." In: *World Environmental and Water Resources Congress 2019: Watershed Management, Irrigation and Drainage, and Water Resources Planning and Management*, ASCE, 264-271. <https://doi.org/10.1061/9780784482339.027>

- Dietz, M. E. (2007). "Low impact development practices: A review of current research and recommendations for future directions." *Water, air, and soil pollution*, 186(1-4), 351–363.
- Dietz, M. E., and Clausen, J. C. (2005). "A field evaluation of rain garden flow and pollutant treatment." *Water, Air, and Soil Pollution*, 167(1-4), 123–138.
- Fu, B. J., Zhao, W. W., Chen, L. D., Liu, Z. F., and Lü, Y. H. (2005). "Eco-hydrological effects of landscape pattern change." *Landscape and Ecological Engineering*, 1(1), 25–32.
- Gallagher, M. T., Snodgrass, J. W., Ownby, D. R., Brand, A. B., Casey, R. E., and Lev, S. (2011). "Watershed-scale analysis of pollutant distributions in stormwater management ponds." *Urban Ecosystems*, 14(3), 469–484.
- Hess, A., Wadzuk, B., and Welker, A. (2017). "Evapotranspiration in rain gardens using weighing lysimeters." *Journal of Irrigation and Drainage Engineering*, 143(6), 04017004.
- Hostetler, M. (2009). "Conserving biodiversity in subdivision development." *University of Florida, Gainesville*, 71–80.
- Ishimatsu, K., Ito, K., Mitani, Y., Tanaka, Y., Sugahara, T., and Naka, Y. (2017). "Use of rain gardens for stormwater management in urban design and planning." *Landscape and Ecological Engineering*, 13(1), 205–212.
- Kansal, M. L., Osheen, & Tyagi, A. (2019). "Hotspot Identification for Urban Flooding in a Satellite Town of National Capital Region of India." In: *World Environmental and Water Resources Congress 2019: Emerging and Innovative Technologies and International Perspectives*, ASCE, 12–24.
- Kim, M. H., Sung, C. Y., Li, M. H., and Chu, K. H. (2012). "Bioretention for stormwater quality improvement in Texas: Removal effectiveness of *Escherichia coli*." *Separation and Purification Technology*, 84, 120–124.
- Li, J., Li, Y., and Li, Y. (2016). "SWMM-based evaluation of the effect of rain gardens on urbanized areas." *Environmental Earth Sciences*, 75(1), 17.
- Osheen, and Singh, K.K. (2019). "Rain Garden—A Solution to Urban Flooding: A Review." In: Agnihotri A., Reddy K., Bansal A. (eds) *Sustainable Engineering. Lecture Notes in Civil Engineering*, vol 30, pp. 27–35. Springer. https://doi.org/10.1007/978-981-13-6717-5_4
- Palhegyi, G. E. (2009). "Modeling and sizing bioretention using flow duration control." *Journal of Hydrologic Engineering*, 15(6), 417–425.
- Penniman, D. C., Hostetler, M., Borisova, T., and Acomb, G. (2013). "Capital cost comparisons between low impact development (LID) and conventional stormwater management systems in Florida." *Suburban Sustainability*, 1(2), 1.
- Swain, S. (2017). "Hydrological Modeling through Soil and Water Assessment Toolin a Climate Change Perspective- A Brief Review." In: *2nd International Conference for Convergence in Technology (I2CT) 2017*, IEEE, 358-361. <https://doi.org/10.1109/I2CT.2017.8226151>
- Swain, S., Dayal, D., Pandey, A., and Mishra, S. K. (2019a). "Trend Analysis of Precipitation and Temperature for Bilaspur District, Chhattisgarh, India." In: *World Environmental and Water Resources Congress 2019: Groundwater, Sustainability, Hydro-Climate/Climate Change, and Environmental Engineering*, ASCE, 193-204. <https://doi.org/10.1061/9780784482346.020>
- Swain, S., Mishra, S. K., and Pandey, A. (2019b). "Spatiotemporal Characterization of Meteorological Droughts and Its Linkage with Environmental Flow Conditions." In: *AGU Fall Meeting 2019*, AGU.
- Swain, S., Nandi, S., and Patel, P. (2018a). "Development of an ARIMA Model for Monthly Rainfall Forecasting over Khordha District, Odisha, India." In: P. K. Sa, S. Bakshi, I. K.

- Hatzilygeroudis, and M. N. Sahoo (eds). *Recent Findings in Intelligent Computing Techniques. Advances in Intelligent Systems and Computing*, Vol. 708, pp. 325-331. Springer, Singapore. https://doi.org/10.1007/978-981-10-8636-6_34
- Swain, S., Patel, P., and Nandi, S. (2017a). "A multiple linear regression model for precipitation forecasting over Cuttack district, Odisha, India." In: *2nd International Conference for Convergence in Technology (I2CT) 2017*, IEEE, 355-357. <https://doi.org/10.1109/I2CT.2017.8226150>
- Swain, S., Patel, P., and Nandi, S. (2017b). "Application of SPI, EDI and PNPI using MSWEP precipitation data over Marathwada, India." In: *IEEE International Geoscience and Remote Sensing Symposium (IGARSS)*, 5505-5507. <https://doi.org/10.1109/IGARSS.2017.8128250>
- Swain, S., Verma, M. K., and Verma, M. K. (2018b). "Streamflow Estimation Using SWAT Model Over Seonath River Basin, Chhattisgarh, India." In: V. P. Singh, S. Yadav, and R. Yadava. (eds). *Hydrologic Modeling. Water Science and Technology Library*, vol. 81, pp. 659-665. Springer, Singapore. https://doi.org/10.1007/978-981-10-5801-1_45
- Tang, S., Luo, W., Jia, Z., Liu, W., Li, S., and Wu, Y. (2016). "Evaluating retention capacity of infiltration rain gardens and their potential effect on urban stormwater management in the sub-humid loess region of China." *Water resources management*, 30(3), 983–1000.
- TRCA. (2008). "Performance evaluation of permeable pavement and a bioretention swale—Seneca College, King City, Ontario." *Toronto and Region Conservation Authority*, Toronto.
- Van Meter, R. J., Swan, C. M., and Snodgrass, J. W. (2011). "Salinization alters ecosystem structure in urban stormwater detention ponds." *Urban Ecosystems*, 14(4), 723–736.
- Wu, J. (2010). "Urban sustainability: an inevitable goal of landscape research." *Landscape Ecology*, 25, 1–4.
- Yang, H., McCoy, E. L., Grewal, P. S., and Dick, W. A. (2010). "Dissolved nutrients and atrazine removal by column-scale monophasic and biphasic rain garden model systems." *Chemosphere*, 80(8), 929–934.
- Yuan, J., Dunnett, N., and Stovin, V. (2017). "The influence of vegetation on rain garden hydrological performance." *Urban Water Journal*, 14(10), 1083–1089.

A Multi-Faceted CFD Evaluation of an Existing Secondary Clarifier

Jordan M. Wilson, Ph.D., A.M.ASCE¹; Carrie L. Knatz, P.E., M.ASCE²;
and J. Alex McCorquodale, Ph.D., P.E.³

¹CDM Smith, Nashville, TN. E-mail: WilsonJ@cdmsmith.com

²Principal, CDM Smith, Carlsbad, CA. E-mail: KnatzCL@cdmsmith.com

³Professor Emeritus, Dept. of Civil Engineering, Univ. of New Orleans, New Orleans, LA. E-mail: jmccorqu@uno.edu

ABSTRACT

As part of the Great Lakes Water Authority's Water Resource Recovery Facility Comprehensive Regional Wastewater Master Plan, computational fluid dynamics (CFD) modeling was used to evaluate the performance and capacity of an existing secondary clarifier. The hydraulic performance was evaluated using three-dimensional (3D) CFD models, and process performance was evaluated using a two-dimensional (2D) CFD model. The clarifier inlet configuration is very complex and unique, where flow is conveyed into the circular clarifiers from a series of diffuser pipes around the periphery. To accurately represent flow into the clarifier from the diffusers, it was essential that the flow through the diffuser be modeled. Modeling flow through each of the 73 inlet diffusers and the clarifier simultaneously proved to be impractical considering the computational resource requirements. Therefore, two separate 3D CFD models were created for a single inlet diffuser and the entire secondary clarifier. The high-resolution single inlet diffuser model was used to both determine and define the inlet boundary conditions of the clarifier model. The velocity field and shear flocculation potential predicted by the 3D CFD models were considered as well as the 2D CFD simulations, which included sludge characteristics and density currents to predict clarifier process performance and capacity. In this paper, the multi-faceted CFD evaluation used to determine the future capacity potential for the GLWA WRRF secondary clarifiers will be discussed. Overall, the model results indicated the performance of the existing secondary clarifiers would not be compromised with an increased surface overflow rate. The paper will detail the approach and results that led to that conclusion.

INTRODUCTION

The Great Lakes Water Authority's (GLWA's) Water Resource Recovery Facility (WRRF) accepts flow from three main interceptors and treats an average of 28.5 cubic meters per second (cms) [650 million gallons per day (mgd)] of wastewater. A large portion of the service area is served by combined sewers. The peak primary treatment capacity for wet weather flows is 74.5 cms (1,700 mgd) and the peak secondary treatment capacity is 40.7 cms (930 mgd). Flow in excess of the secondary treatment capacity receives primary treatment and disinfection prior to discharge. The WRRF began operation in 1940 as a primary treatment facility which provided dewatering and incineration of the primary sludge. In the 1970's, the facility was upgraded to provide secondary treatment with an oxygen activated sludge system. Remote facilities were installed in the collection system in the 1990's in order to remove floatables and to provide sedimentation and disinfection to combined sewer overflow outfalls prior to discharge to the receiving waters.

PURPOSE AND OBJECTIVES

The GLWA WRRF has twenty-five (25) 30.5-meter (200-foot) diameter circular secondary clarifiers. As part of ongoing improvements at the facility, GLWA decided to perform an evaluation of the current secondary clarifier performance in order to determine if the clarifiers could be operated at a higher overflow rate, and in turn, increase the reliability and redundancy of the system. The secondary clarifiers were evaluated with a field-testing campaign, as well as with three-dimensional (3D) and two-dimensional (2D) computational fluid dynamics (CFD) simulations. The purpose of the 3D CFD analysis was to evaluate the flow distribution and flocculation potential of an existing secondary clarifier. Figure 1 displays one of the 25 secondary clarifiers dewatered for inspection and evaluated in the analysis presented herein. Flow is conveyed into the clarifiers from a series of diffuser pipes around the periphery. Clarified effluent flow passes under the scum baffle and into the effluent troughs.

The 3D CFD analysis developed a baseline simulation of the existing clarifier to serve as a reference for future simulations that would assess clarifier performance after potential modifications. The objectives of the 3D CFD analysis were to understand the flow field using velocity streamlines, to identify the average velocity gradient or shear flocculation potential, G , within the clarifier, and to determine the potential capacity of the clarifier. The purpose of the 2D CFD analysis was to predict clarifier effluent total suspended solids (TSS) as a function of surface overflow rate (SOR) and predict the return and waste activated sludge concentration as well as sludge blanket depth.

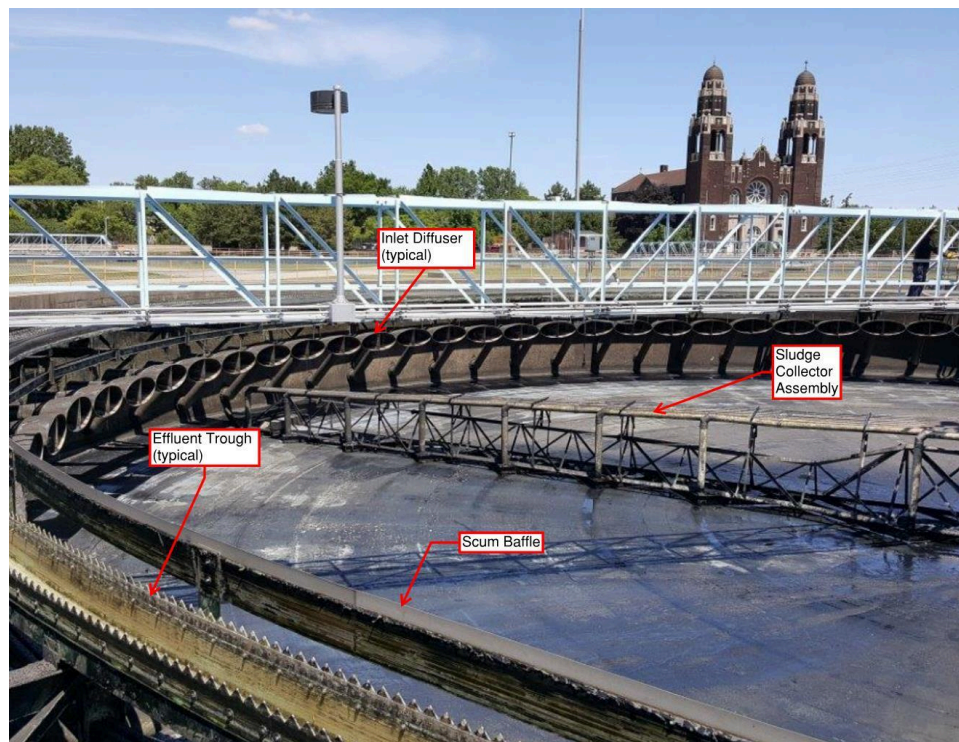


Figure 1. GLWA WRRF Secondary Clarifier.

THEORY

Inflow uniformity and the potential for re-entrainment of clarified liquid into the influent was

evaluated based on comparisons of velocity profiles. It is understood that the highest potential for shear flocculation is in areas with a G value within the range of 30 to 70 s^{-1} (J. A. McCorquodale, personal communication, October 24, 2017). Further, *WEF Manual of Practice No. FD-8* identifies typical G values for flocculation between 10 and 75 s^{-1} (WEF 2005). G values were used to evaluate the energy dissipation and flocculation conditions. The shear flocculation potential, G , parameter was used in the analysis. For hydraulic flocculation, the average velocity gradient can be calculated by:

$$G = \sqrt{\frac{\rho gh}{\mu t}}, \quad \text{Equation 1}$$

where ρ is the density (kg/m^3), g is the gravitational constant (m/s^2), h is the headloss (m), μ is the dynamic viscosity ($N\cdot s/m^2$), and t is the retention time (s) (Bridgeman, Jefferson, and Parsons 2010). Camp and Stein (1943) also showed that the average velocity gradient can be written in terms of power dissipation per unit of mass as:

$$G = \sqrt{\frac{\bar{\varepsilon}}{\nu}}, \quad \text{Equation 2}$$

where $\bar{\varepsilon}$ is the average power dissipation (m^2/s^3) and ν is the kinematic viscosity (m^2/s). CFD provides the ability to investigate G at any point in the model domain substituting the turbulent kinetic energy dissipation rate, ε , for $\bar{\varepsilon}$ (Bridgeman, Jefferson, and Parsons 2010) which results in the following:

$$G = \sqrt{\frac{\varepsilon}{\nu}}. \quad \text{Equation 3}$$

Equation 3 serves as the basis for calculation of G in this analysis.

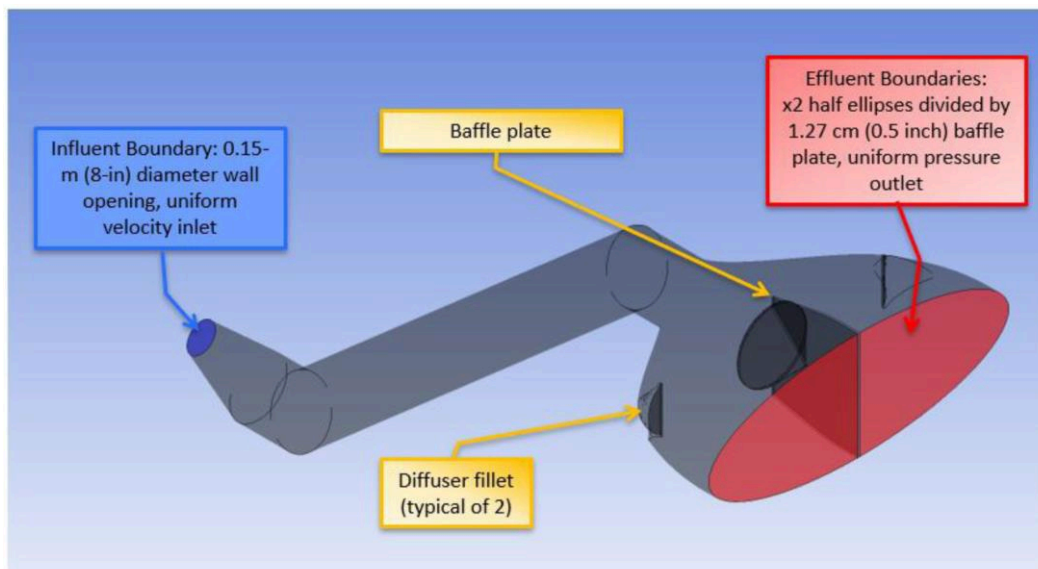


Figure 2. GLWA Secondary Clarifier Diffuser Model Geometry.

MODEL METHODOLOGY

3D CFD Models: The 3D CFD models used for GLWA were developed using Ansys Workbench 18.2. This platform includes SpaceClaim to develop the model geometry, Ansys Mesher to generate the mesh, Ansys Fluent for model processing and post-processing, and CFD-

Post for post-processing. The models were setup for a single-phase (water), steady-state analysis in order to simulate the flow through the clarifier. The realizable k - ϵ model was used to model flow turbulence (Shih 1995). This turbulence model solves for two separate transport equations: turbulent kinetic energy, k or TKE hereafter, and the turbulent kinetic energy dissipation rate, ϵ . The models were run for specified flow rates of 1.3 cms (29 mgd), 1.8 cms (40 mgd), and 2.4 cms (54 mgd) with a constant return activated sludge (RAS) of 0.3 cms (7 mgd). The secondary clarifiers at the GLWA WRRF have a unique inlet geometry due to the peripheral diffuser pipes. To accurately represent flow into the clarifier from the diffusers, the flow through the diffuser needed to be modeled. Modeling flow through each of the 73 diffusers, and the entire clarifier simultaneously, was impractical considering the computational resource requirements. Therefore, two separate models were created where the effluent velocity profile from the single diffuser model was defined as the influent velocity profile in order to represent each of the 73 diffusers in the secondary clarifier model.

3D Single Diffuser Model: Figure 2 illustrates the 3D single diffuser model geometry and boundary conditions. The single diffuser model includes an 0.15-meter (8-inch) to 0.41-meter (16-inch) eccentric expansion, a 0.41-meter (16-inch) connector pipe, and a 2.13-meter (7.0-foot) by 0.76-meter (2.5-foot) elliptical diffuser outlet structure with a minimum radius of 0.76 meter (2.5 feet) and a maximum radius of 2.13 meter (7.0 feet). The diffuser outlet structure also includes axial and radial diffuser plates and diffuser fillets. The simulations considered minimum, average, and maximum flow conditions of 1.3 cms (29 mgd), 1.8 cms (40 mgd), and 2.4 cms (54 mgd), respectively. The diffuser inlet is treated as a uniform velocity inlet, and the outlet is a pressure outlet with a static pressure of 0 pascal. Turbulence boundary conditions are prescribed for the hydraulic diameter and turbulence intensity.

3D Secondary Clarifier Model: Figure 3 illustrates the 3D secondary clarifier model geometry, for which the single diffuser model was used to inform the inlet boundary conditions. Velocity, turbulent kinetic energy, and turbulent dissipation rate profiles were extracted from the diffuser model and prescribed to the diffuser outlet faces within the clarifier domain. The RAS effluent boundaries were assumed velocity outlets at the established RAS flow rate. The weir effluent boundaries were treated as pressure outlets with a static pressure of 0 pascal. To efficiently model the clarifier, geometry simplifications were made to the effluent weir configuration. The v-notch weirs along the perimeter of the weir troughs were modeled as sharp-crested weirs.

The diffuser piping was included in the clarifier model geometry as a void space in the clarifier, since the outlet of the diffuser is the inlet boundary of the clarifier model. Based on record drawings, 70 of the 73 diffusers have straight piping and three diffusers have skewed piping in order to accommodate the scum collector box. Although the individual diffuser model was based on the straight pipe configuration, the effect of the skewed piping on the velocity and turbulence fields at the diffuser outlets was considered negligible to the overall hydraulics of the clarifier. As such, the profile for the straight diffuser was also used as the boundary condition for the skewed diffusers.

2D CFD Model: 2-Dimensional circular (customized 2Dc, McCorquodale et al. 2005) CFD software was used to evaluate the process performance for this analysis. Although this model assumes flow through the clarifier is circumferentially invariant, the 3D model indicated three-dimensional flow especially in the inlet zone, and the 3D CFD models provided an understanding of the hydraulic conditions for the actual clarifier. The 2D model provided help to visualize the density currents and sludge blanket processes.